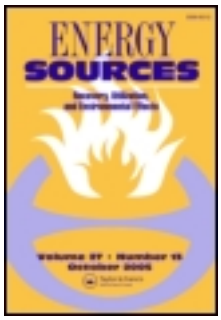

Energy Sources, Part A: Recovery, Utilization, and Environmental Effects

Publication details, including instructions for authors and subscription information:
http://www.tandfonline.com/loi/ueso20

Diffusive and Convective Mechanisms during CO_2 Sequestration in Aquifers

E. Ozgur [a] & F. Gumrah [a]

[a] Petroleum and Natural Gas Engineering Department, Middle East Technical University, Ankara, Turkey

Available online: 17 Mar 2009

To cite this article: E. Ozgur & F. Gumrah (2009): Diffusive and Convective Mechanisms during CO_2 Sequestration in Aquifers, Energy Sources, Part A: Recovery, Utilization, and Environmental Effects, 31:8, 698-709

To link to this article: http://dx.doi.org/10.1080/15567030701743668

Energy Sources, Part A, 31:698–709, 2009

ISSN: 1556-7036 print/1556-7230 online
DOI: 10.1080/15567030701743668

Taylor & Francis
Taylor & Francis Group

Diffusive and Convective Mechanisms during CO_2 Sequestration in Aquifers

E. OZGUR[1] and F. GUMRAH[1]

[1]Petroleum and Natural Gas Engineering Department, Middle East Technical University, Ankara, Turkey

Abstract *CO_2 emissions originated from industrial sources can be captured, transported, and stored in depleted gas/oil fields and deep saline aquifers. The transport mechanisms, occurred during CO_2 sequestration in deep saline aquifers, are examined in this study. After injecting CO_2 until the tolerable pressure for the aquifer is reached, the wells are closed and CO_2 is deposited as free gas and soluble gas in water under the sealing rock. During injection and waiting periods, the concentration profile of CO_2 within the aquifer is formed by diffusion and convection mechanisms. The Rayleigh number and mixing zone length concepts are used for investigating the effect of reservoir properties, such as dispersivity, permeability, porosity, and others on the aforementioned mechanisms. The results of convective dominant mechanism in aquifers with 1 md and 10 md permeability values are so near in that diffusion-dominated system. After 10 md, the convection mechanism begins to dominate gradually and it becomes totally convection dominated for 50 md and higher permeability values. These results are also verified by the Rayleigh number and mixing zone lengths.*

Keywords analytical modeling, CO_2 sequestration, convection, deep saline aquifer, diffusion, numerical modeling

Introduction

Global warming is one of the most important environmental problems facing the world. It is widely considered to be caused by an atmospheric greenhouse effect. The contribution of CO_2 to this greenhouse effect is estimated to equate approximately to 50% of the effect of all greenhouse gases together, making the reduction of CO_2 emissions an important goal. The global warming may cause disruption in the chemical composition and physical dynamics of the Earth's atmosphere, leading to the distribution of heat or energy around atmosphere abnormally (Justus and Fletcher, 2006).

Sources of anthropogenic CO_2 can be centralized, as in a power generating station, or diffuse, as in the use of motor vehicles. The concentration of CO_2 in the atmosphere is rising and, due to growing concern about its effects, the U.S. and over 160 other countries ratified the Rio Mandate in 1992, which calls for "... stabilization of greenhouse gas

Address correspondence to Prof. Dr. Fevzi Gumrah, Middle East Technical University, Petroleum and Natural Gas Engineering Department, İnönü Bulvarı, Ankara 06531, Turkey. E-mail: fevzi@metu.edu.tr

concentrations in the atmosphere at a level that would prevent dangerous anthropogenic interference with the climate system." Reduction of anthropogenic CO_2 emissions into the atmosphere can be achieved by a variety of means, which has been summarized by Herzog (1998). Three methods can be employed, i.e., reducing energy intensity, reducing carbon intensity, and carbon sequestration.

Carbon dioxide sinks can be grouped into three broad classes based on the nature, location, and ultimate fate of CO_2. These groupings are as follows: *Biosphere sinks* are active and environmentally sensitive, natural reservoirs for CO_2. The oceans, forests, and soils (agricultural) ecosystems are members of this class. *Geosphere sinks* are natural reservoirs for CO_2 but require anthropogenic intervention in order to make use of the sink. Members of this class include oil reservoirs suitable for enhanced oil recovery (EOR), coal beds, depleted oil and gas reservoirs, and deep aquifers. *Material sinks* are anthropogenically created/generated pools of carbon. Members of this class include durable wood products, chemicals, and plastics.

Carbon-dioxide disposal into low permeability, deep aquifers in sedimentary basins have been shown to be technically feasible as geologic sinks and offer the largest potential for the landlocked areas of the world. Deep aquifers contain high salinity water and could host large amounts of CO_2 trapped by the formation pressure. The determining factors are the pressure and temperature in the reservoir. At reservoir depths of 800 m and greater, the temperature and pressure of the CO_2 would be above the supercritical condition, which is desirable from a storage perspective. Aquifers suitable for injection of CO_2 must satisfy the following general conditions: the top of the aquifer must be greater than 800 m below ground level; the aquifer should be capped by a regional aquitard (sealing unit); the aquifer should have enough porosity and adequate permeability; and the injection site should be close to the CO_2 emitting source (Bachu et al., 1994).

Hassanzadeh et al. (2005) studied the diffusive and convective mixing in geological storage of CO_2 with numerical model. Depending on the system Rayleigh number and the formation heterogeneity, convective mixing greatly accelerated the dissolution of CO_2 in an aquifer. More than 60% of the ultimate dissolution was achieved after 800 years based on the Nisku aquifer problem.

Bachu and Carroll (2005) studied the CO_2 injection into a saline reservoir that is 40–60% denser than CO_2. Driven by density contrasts, CO_2 will flow horizontally (in a horizontal aquifer) spreading under the caprock, and flow upwards, potentially leaking through any high permeability zones or artificial penetrations, such as abandoned wells. The free-phase CO_2 (usually supercritical fluid) slowly dissolves in the brines. The resulting CO_2-rich brines are slightly denser than undersaturated brines, making them negatively buoyant, and thus greatly reducing or eliminating the possibility of leakage.

The rate of dissolution depends on the rate at which diffusion or convection brings undersaturated brine in contact with CO_2. Convective mixing enhances the dissolution rate as compared to diffusion by distributing the CO_2 into the aquifer (Lindeberg and Wessel-Berg, 1996). Therefore, the role of convective mixing in CO_2 sequestration and the timescales involved in the process are important. The dissolution time of the injected CO_2 into brine is important because during this time the injected CO_2 has a chance to leak into the atmosphere through the caprock and wellbores (Hassanzadeh et al., 2005).

In this study, the transport of CO_2 dissolved in brine is examined by molecular diffusion and mechanical dispersion mechanisms in the solubility trapping part. The effect of aquifer properties on the transportation of injected CO_2 is analyzed with analytical modeling approach using the Rayleigh number and mixing zone length concepts.

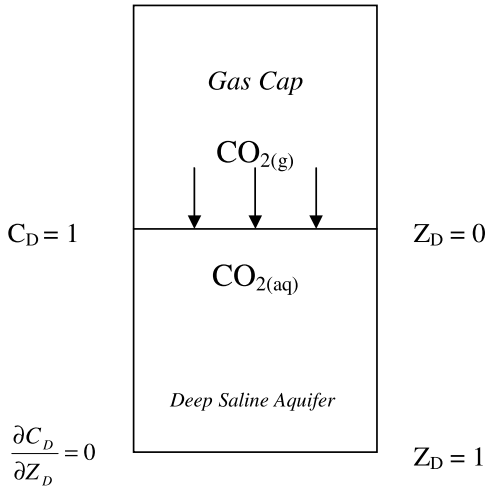

Figure 1. Geometry and boundary conditions of the model ($H = 100$ m).

Diffusive and Convective Mixing

The hypothetical model (Figure 1) is created with some assumptions. There is a CO_2 cap formed above the aquifer and the CO_2 pressure is kept at a constant value throughout the modeling as a top boundary. The aquifer system is assumed as isothermal condition. The possible geochemical reactions that can reduce the timescale of sequestration of CO_2 are not included, since they generally occur on longer timescales (Gunter et al., 1997). The CO_2 diffuses into brine in a one-dimensional vertical system. The density of brine increases with an increase in CO_2 saturation. The density difference results from the convective movement of brine within the aquifer. Analytical solutions for diffusive and convective equation are used first for determining CO_2 concentrations in brine to calculate the mixing zone lengths and for estimating brine velocities to obtain Rayleigh numbers. The common data to be used in the analytical model are given in Table 1.

Table 1
Common data to all runs given in Tables 2 and 3

Data	Value
Aquifer thickness, m	100
Viscosity of water, cp	0.7
Temperature, °C	50
Pressure, atm	75
Aquifer top, m	850
Aquifer bottom, m	950
Molecular diffusion coefficient of CO_2 in water, cm^2/s	3.10^{-5}

The behavior of diffusion dominant process in the aquifer could be expressed with the equation known as Fick's diffusion equation (1):

$$D_e \frac{\partial^2 c}{\partial z^2} = \frac{\partial c}{\partial t}. \tag{1}$$

The effects of porosity and tortuosity are combined together in the definition of an effective molecular diffusion coefficient (D_e) in Eq. (2):

$$D_e = \frac{D_o \phi}{\tau}, \tag{2}$$

in which D_e is the effective diffusion coefficient within pores, D_o is the molecular diffusion coefficient within pores, ϕ is porosity, and τ is the tortuosity. The analytical solution of Eq. (1) is given in Eq. (3). The run conditions for diffusion-dominated systems are given in Table 2:

$$\frac{C(z,t)}{C_o} = erfc\left[\frac{z}{2\sqrt{D_e.t}}\right]. \tag{3}$$

In the aquifer, molecular diffusion normally forms due to the concentration difference in brine. The concentration difference or density difference in brine triggers the convection mechanism and the velocity of brine is determined from Eq. (4):

$$u = \frac{k.g.\Delta\rho}{\mu}. \tag{4}$$

In a vertical convection system, the velocity term is added to the Fick's diffusion equation (1) and Eq. (5) is used as a diffusion-convection equation:

$$D_e \frac{\partial^2 c}{\partial z^2} - \frac{u}{\phi}\frac{\partial c}{\partial z} = \frac{\partial c}{\partial t}, \tag{5}$$

Table 2
Run conditions for analytical modeling with only molecular diffusion

Run cases	Time, y	Porosity, fraction
1a	5,000	0.2
1b	10,000	0.2
1c	20,000	0.2
1d	100,000	0.2
1e	10,000,000	0.2
2a	20,000	0.1
2b	20,000	0.3

where the effective diffusion coefficient for convection-dominated systems is

$$D_e = \frac{D_o.\phi}{\tau} + \alpha.v. \tag{6}$$

Equation 5 could be arranged in dimensionless form to make the equation unique with given boundary conditions as in Eq. (7) (Lake, 1989):

$$\frac{1}{N_{Pe}} \frac{\partial^2 C_D^2}{\partial Z_D^2} - \frac{\partial C_D}{\partial Z_D} = \frac{\partial C_D}{\partial t_D}, \tag{7}$$

where the dimensionless groups are:

$$C_D = \frac{C_{CO_2}}{C_{CO_2,sat}}, \tag{8}$$

$$Z_D = \frac{z}{H}, \tag{9}$$

$$t_D = \frac{u.t}{\phi.H}, \tag{10}$$

$$N_{Pe} = \frac{u.H}{\phi.D_e}. \tag{11}$$

The initial and boundary conditions are also defined in the hypothetical model for solving the problem.

Initial condition:

$$C_D = 0 \text{ for } t_D = 0 \text{ and for all } Z_D \tag{12}$$

Boundary conditions:

$$\text{At } Z_D = 0\text{: } C_D = 1 \text{ for } t_D > 0 \tag{13}$$

$$\text{At } Z_D = 1\text{: } \frac{\partial C_D}{\partial Z_D} = 0 \tag{14}$$

For the given boundary conditions in Eqs. (12), (13), and (14), the final dimensionless CO_2 concentration becomes as in Eq. (15), which is an exact analytic solution for Eq. (3) (Lake, 1989):

$$C_D = \frac{1}{2} erfc\left(\frac{z_D - t_D}{2\sqrt{\frac{t_D}{N_{Pe}}}}\right) + \frac{e^{z_D N_{Pe}}}{2} erfc\left(\frac{z_D + t_D}{2\sqrt{\frac{t_D}{N_{Pe}}}}\right) \tag{15}$$

To find the necessary concentration values in mixing zone length, Eq. (3) is used for the diffusion-dominated system and Eq. (15) is used for the convection-dominated system. The run conditions for the convection-dominated system are given in Table 3.

Table 3
Run conditions for analytical modeling with dispersion

Run cases	Dispersivity, m	Permeability, md	Porosity, fraction	Time, y
3a	1	100	0.2	200
3b	10	100	0.2	200
3c	20	100	0.2	200
4a	1	100	0.2	750
4b	10	100	0.2	750
4c	20	100	0.2	750
5a	1	100	0.2	6,000
5b	10	100	0.2	6,000
5c	20	100	0.2	6,000
6a	10	1	0.2	1,000
6b	10	10	0.2	1,000
6c	10	100	0.2	1,000
6d	10	1,000	0.2	1,000
7a	10	100	0.1	200
7b	10	100	0.3	200

CO_2 Saturated Part of the Aquifer

The CO_2 saturated part of the aquifer is calculated by integrating all C_D vs. Z_D curves obtained from analytical models. The CO_2 saturated part of the aquifer is determined in the dimensionless unit. It can be considered as a fraction of total aquifer volume:

$$\text{CO}_2 \text{ saturated part of the aquifer (fraction)} = \int_0^{Z_{D\,(\max)}} C_D.dZ_D \tag{16}$$

Determination of Mixing Zone Lengths

The dimensionless mixing zone length, Eq. (17), is defined as the difference between two points where $C_D = 0.1$ and $C_D = 0.9$ (Lake, 1989). This is the fraction of the total system length that lies between defined concentration limits at a given time. The analytical model is only used to find the mixing zone lengths. Some run cases (Run 1e, 5a, 5b, 5c, and 6d) are omitted due to the lowest value of C_D being lower than 0.1 and the greatest value of C_D being higher than 0.9, which is out of definition in dimensionless mixing zone:

$$\Delta z_D = z_D|_{C_D=0.1} - z_D|_{C_D=0.9}. \tag{17}$$

Rayleigh Number and Peclet Number

The rising of convection could be comprehended by the dimensionless solutal Rayleigh number (Eq. (18)). The Rayleigh number encompasses parameters that form a velocity term. For a fluid layer between the constant concentration top boundary and the impermeable bottom boundary, the critical solutal Rayleigh number has been calculated in

theory to be $4\pi^2$ (around 39.48) for the occurrence of convection process (Weatherill et al., 2004). If the Rayleigh number is over this critical number, convection takes place:

$$Ra = \frac{kg\Delta\rho H}{D_o\mu\phi} = \frac{uH}{D_o\phi}. \tag{18}$$

Peclet numbers for each run are calculated with Eq. (11). The Peclet number gives the ratio of convective forces to dispersive forces.

Results and Discussion

The data to be used in analytical modeling are given in Tables 1, 2, and 3. Equation (3) is used for the solution of the cases in which only the molecular diffusion mechanism is considered. When the porosity of aquifer increases, the effective diffusion coefficient of solute in the brine increases. So, the diffusion rate is higher at higher porosity systems and the aquifer with higher porosity is saturated with CO_2 faster. Figure 2 is given as an example for illustrating the CO_2 concentration profile in an aquifer for the diffusion-dominated process. The dissolved amount of CO_2 increases with time. However, due to the diffusion-dominated system the dissolution rate is very slow. Even after 10,000,000 years the aquifer is not fully saturated with CO_2.

In the convection dominant process, Eq. (15) is used for the solution of the run cases. When the dispersivity increases, more CO_2 is spread through the aquifer in an early time region (200 years). In the middle time region (750 years), at the top of the aquifer more CO_2 is accumulated with lower dispersivity values for aquifers. After a point, this turns out to be opposite and more CO_2 is accumulated at the deeper parts of the aquifer for higher dispersivity as in the early time region. At the end of the dissolution process in the aquifer, the dissolved CO_2 amount in the aquifer increases with lower dispersivity values for the late time region (6,000 years). Although the dissolved CO_2 amount is more in the early time of the whole transport in higher dispersivity value, the complete dissolution takes place earlier in lower dispersivity value. As the permeability of the aquifer increases, the convection rate increases due to increased velocity. The saturated CO_2 amount increases with increased permeability. At low porosity, the convection rate

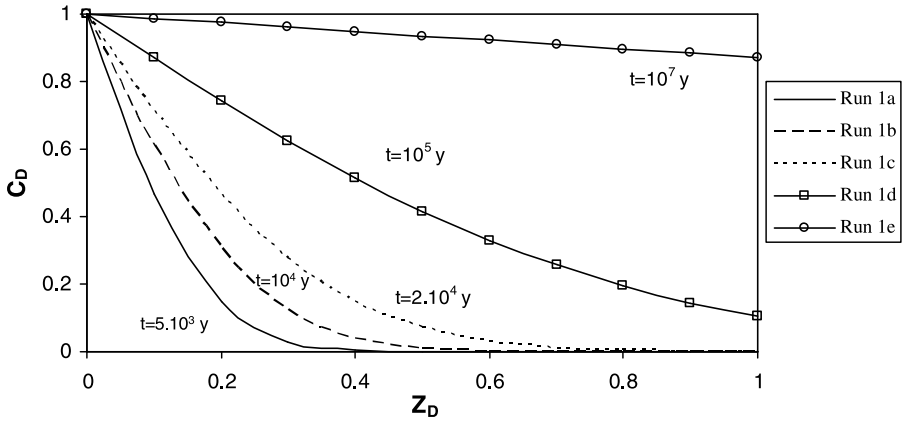

Figure 2. Effect of duration on CO_2 saturation ($\varnothing = 0.2$, analytical model).

is faster due to higher interstitial velocity. So, with an increase in porosity the convection rate of the transport decreases.

The CO_2 saturated part of the aquifer is calculated by integrating Eq. (16) and the results are given in Table 4.

After obtaining CO_2 concentrations in brine for all cases, the following mixing zone lengths are calculated by using Eq. (17). Then the velocities are calculated for determining Rayleigh numbers.

The mixing zone length increases with time and porosity as seen in Figures 3 and 4, respectively, in the diffusion-dominated system.

In the convection-dominated system, the mixing zone length increases with dispersivity as seen in Figure 5. It increases with permeability after a point as seen in Figure 6. This point is the sign of the beginning of convection in the system. It decreases with porosity as seen in Figure 7.

Rayleigh numbers for each run are calculated with Eq. (18) and presented in Table 4. The Rayleigh number gives an idea about the occurrence of convection. Since the velocity changes in the system as a function of space and time, the average velocities are used for the calculation of Rayleigh numbers. Velocities are calculated based on the geometric mean, which is a measure of central tendency (see Table 5). According to this computation, average velocities are found to be in the range of 0.5–2% of maximum

Table 4
Aquifer saturation amounts, Rayleigh numbers and Peclet numbers

Run cases	CO_2 saturated part of the aquifer, fraction	Rayleigh number	Peclet number
1a	0.12	—	—
1b	0.15	—	—
1c	0.22	—	—
1d	0.46	—	—
1e	0.94	—	—
2a	0.15	—	—
2b	0.27	—	—
3a	0.05	116	9.2
3b	0.12	233	9.6
3c	0.15	233	9.6
4a	0.23	146	9.4
4b	0.2	81	8.9
4c	0.2	58	8.5
5a	0.99	116	9.2
5b	0.95	116	9.2
5c	0.92	116	9.2
6a	0.07	6	3.7
6b	0.08	8	4.5
6c	0.54	233	9.6
6d	1	1,164	9.9
7a	0.31	582	9.8
7b	0.08	77	8.9

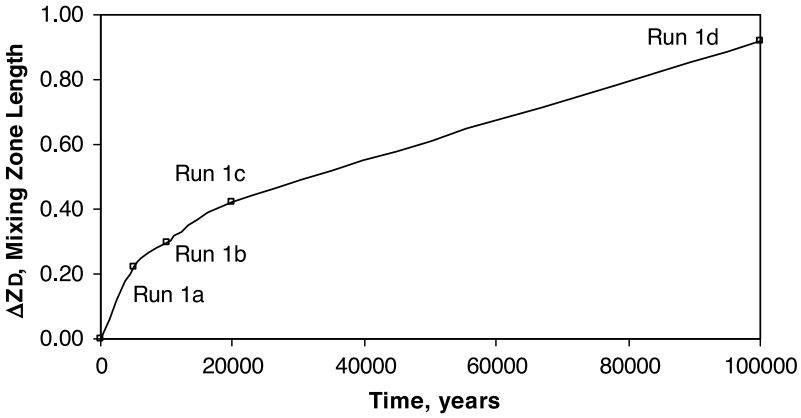

Figure 3. Variation of mixing zone with time for diffusion-dominated system.

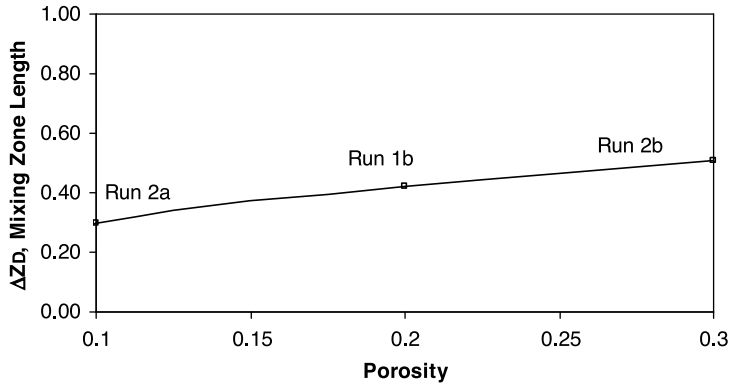

Figure 4. Variation of mixing zone with porosity for diffusion-dominated system (20,000 years).

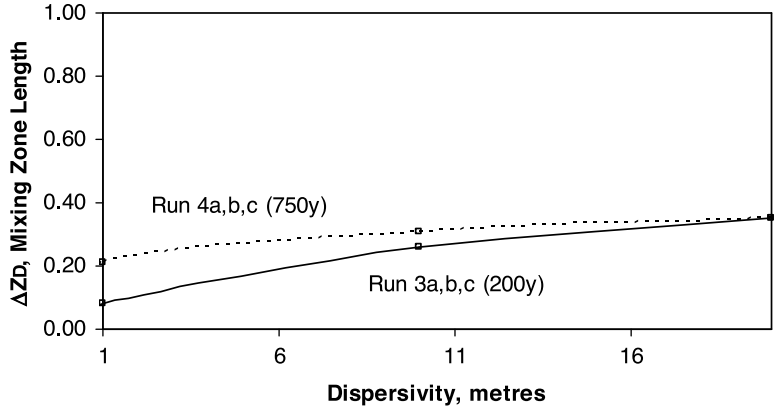

Figure 5. Variation of mixing zone with dispersivity for convection-dominated system.

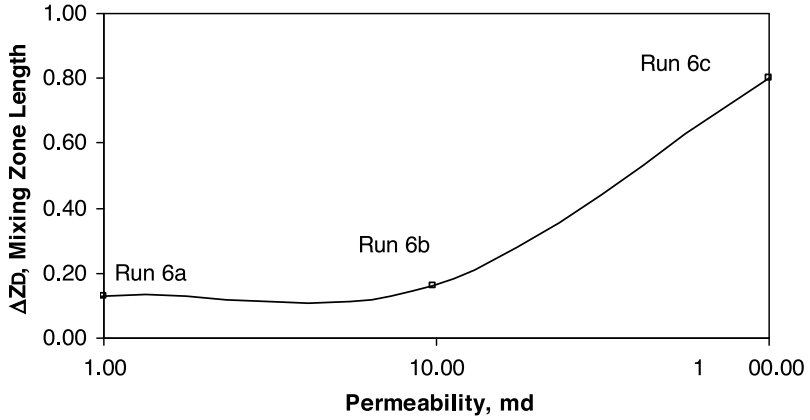

Figure 6. Variation of mixing zone with permeability for convection-dominated system (1,000 years).

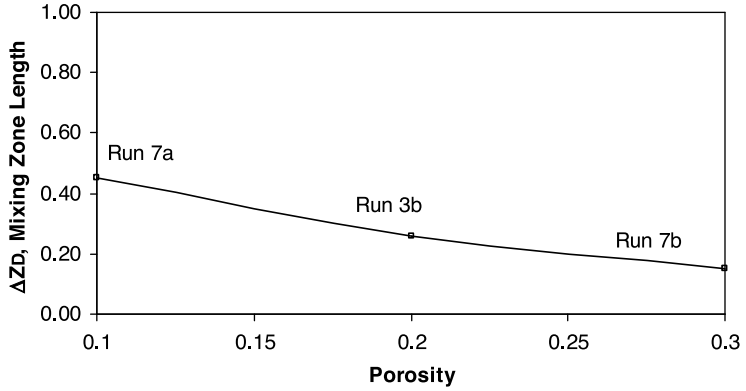

Figure 7. Variation of mixing zone with porosity for convection-dominated system (200 years).

Table 5
Maximum velocities occurred in the runs

Run cases	Maximum velocity, cm/s
3a, 3b, 3c	7.01×10^{-6}
4a, 4b, 4c	7.01×10^{-6}
5a, 5b, 5c	7.01×10^{-6}
6a	7.01×10^{-8}
6b	7.01×10^{-7}
6c	7.01×10^{-6}
6d	7.01×10^{-5}
7a	1.40×10^{-5}
7b	4.67×10^{-6}

velocities. The maximum velocity values in Table 5 are in the order 10^{-5} cm/s and 10^{-8} cm/s in run cases, as calculated with Eq. (4). As seen in Table 4, Rayleigh numbers of runs 6a and 6b are below the critical Rayleigh number which is about 39.5.

Peclet numbers for each run are calculated with Eq. (11) and given in Table 4. Peclet numbers are nearly the same for each run except for runs 6a and 6b in which the diffusion mechanism is dominated.

Conclusions

The effects of aquifer properties on transport mechanisms are evaluated in a one-dimensional vertical system. The following remarks are concluded:

- In the diffusion-dominant process, dissolution of CO_2 in the aquifer increases with porosity; however, in the convection-dominant process dissolution of CO_2 in aquifer decreases with porosity. Because of this, the increase in porosity decreases the velocity of brine in the aquifer.
- The increase in permeability accelerates the dissolution of CO_2 in aquifer significantly, which might be due to increasing velocity.
- Dispersivity increases the spreading and the transport distance of CO_2 in the aquifer. At the end of the dissolution process in the aquifer, the dissolved CO_2 amount in the aquifer increases with lower dispersivity values.
- The results of convective dominant mechanism in aquifers with 1 md and 10 md permeability values are so near to that of the diffusion-dominated system. After 10 md, the convection mechanism begins to dominate gradually and it becomes totally convection dominated for 50 md and higher permeability values. These results are also verified by the Rayleigh number and mixing zone lengths.

References

Bachu, S., Gunter, W. D., and Perkins, E. H. 1994. Aquifer disposal of CO_2: Hydrodynamic and mineral trapping. *Energy Convers. Mgmt*. 35:269–279.

Bachu, S., and Carroll, J. J. 2006. In-situ phase and thermodynamic properties of resident brine and acid gases (CO_2 and H_2S) injected in geological formations in western Canada. *Proceedings of 7th International Conference on Greenhouse Gas Control Technologies,* Vol. 1, pp. 449–458.

Gunter, W. E., Perkins, E. H., and Wiwchar, B. 1997. Aquifer disposal of CO_2-rich greenhouse gases: Extension of the time scale of experiment for CO_2-sequestering reactions by geochemical modeling. *Mineralogy & Petrology* 59:121–140.

Hassanzadeh, H., Pooladi-Darvish, M., and Keith, D. W. 2005. Modeling of convective mixing in CO_2 storage. *J. Canadian Petrol. Technol.* 44:43–51.

Herzog, H. 1998. Understanding sequestration as a means of carbon management. *US DOE Workshop on Carbon Sequestration at MIT*, Boston, MA, June 22–23, p. 6.

Justus, J. R., and Fletcher, S. R. 2006. Global climate change. Congressional Research Service, March 2006, Report No. RL 33602, Washington, DC: Congressional Research Service.

Lake, L. W. 1989. Enhanced Oil Recovery. Englewood Cliffs, New Jersey: Prentice-Hall.

Lindeberg, E. G. B., and Wessel-Berg, D. 1996. Vertical convection in an aquifer column under a gas cap of CO_2. *Energy Convers. Mgmt.* 38:229–234.

Weatherill, D., Simmons, C. T., Voss, C. I., and Robinson, N. I. 2004. Testing density-dependent groundwater models: Two-dimensional steady state unstable convection in infinite, finite and inclined porous layers. *Adv. Water Res*. 27:547–562.

Nomenclature

α	Dispersivity, cm
μ	Viscosity, g/cm^2.sec
$\Delta\rho$	Density difference, g/cm^3
$\varnothing$	Porosity of reservoir, fraction
τ	Tortuosity
C_{CO_2}	Concentration of CO_2 in aquifer, mol/cm^3
$C_{CO_2,sat}$	Concentration of CO_2 in saturated aquifer at aquifer conditions, mol/cm^3
C_D	Dimensionless concentration
D_e	Effective diffusivity coefficient, cm^2/s
D_o	Molecular diffusion coefficient, cm^2/s
g	Gravitational acceleration, cm/s^2
H	Thickness, cm
k	Permeability, cm^2
N_{Pe}	Peclet number
Ra	Rayleigh number
t	Time, second
t_D	Dimensionless time
u	Superficial velocity, cm/s
v_o	Interstitial velocity, cm/s, $u/\varnothing$
z	Depth below the interface, cm
Z_D	Dimensionless length